DOI: 10.13009/EUCASS2023-985
Aerospace Europe Conference 2023 – 10TH EUCASS – 9TH CEAS

Ionic liquids performance for externally wetted electrospray propulsion system

David Villegas-Prados[⋆*†], *Javier Cruz*[⋆], *Mick Wijnen*[⋆], *Pablo Fajardo*[*], *Jaume Navarro*[*]
[⋆]*IENAI SPACE*
[*]*Universidad Carlos III de Madrid*
Leganés, Madrid
david.villegas@ienai.space
[†]Corresponding author

Abstract

Ionic liquids are the base for electrospray propulsion. We have selected seven liquids to characterize them using an externally wetted electrospray thruster. These are EMI-BF_4, EMI-DCA, EMI-Im, EMI-SCN, EMI-$EtOSO_3$, EMI-OTf and EMI-TFA. This research marks the first time that the latter four liquids are reported for externally wetted emitters. A complete thruster assembly has been tested with each of the propellants. Using time-of-flight mass spectrometry, the performance of these ionic liquids has been characterized, assessing thrust, specific impulse and thrust efficiency. EMI-BF_4, EMI-DCA and EMI-SCN were found to operate in pure ionic regime while EMI-Im, EMI-$EtOSO_3$, EMI-OTf and EMI-TFA operate in mixed regime.

1. Introduction

Electrospray thrusters have emerged as a promising propulsion technology within the EP community, offering unique advantages over electric propulsion devices, such as ion or hall thrusters. These systems are especially well-suited for micro and nano satellites, as they can maintain efficiencies greater than 50% even at power levels below 100 W.[1,2] Moreover, electrospray thrusters are known for their compact size and scalability, making them adaptable to various spacecraft sizes and mission requirements.

The operating principle of electrospray thrusters involves the application of a static electric field to extract and accelerate charged particles from a conductive liquid propellant, generally known as Ionic liquids (ILs). These are molten salts that comprise stable mixtures of positive and negative molecular ions. ILs possess a significant advantage in their exceptionally low vapor pressure, rendering them ideal for space applications. Furthermore, the emission of both positive and negative ions allows for a net neutral emission, eliminating the need for a neutralizer.[3] The propellant coats a substrate, known as the emitter, which is positioned in close proximity to an extractor grid. An electric potential difference is established between the liquid and extractor grid, creating a strong electric field. When the electric field reaches a sufficient intensity, ions can be extracted from the emission sites through the Taylor cone phenomenon.[4] These ions are then accelerated by the electric field, forming a high-speed jet that generates thrust.[5]

Depending on the particles emitted by the thruster two regimes of operation have been reported, oR a mixture of these. The cone-jet or droplet regime is described by the extraction of liquid clusters called droplets.[6] The ionic regime is the pure extraction of ions from the liquid. A mixed regime exist when a combination of droplets and pure ions are present in the plume.[7] The droplet regime is characterized by heavier but slower particles, producing a higher thrust but lower specific impulse compared by the faster and lighter plume produced in ionic regime. In terms of performance, the mixed regime is characterized by a lower efficiency as produced by the presence of the different particles.

The emission regime in which an electrospray operates and its overall performance depend on several factors: the emitter geometry, the applied electric field, the ionic liquid properties and the operation temperature.[8,9] Several types of electrospray thruster exist according to their emitter configuration: capillary,[10] porous[11] and externally wetted emitters.[12] The present study is focused on externally wetted emitters.

In this type of electrospray the liquid flows on top of the emitter surface which features cone-like protrusions. At the tip of the cones, called hereafter emission site, the electric field strength intensifies, and when the surface tension forces are not able to hold the liquid, extraction from the emission site starts taking place. The potential created between the emitter and the extractor accelerates the extracted particles. These type of emitters were first tested with ionic liquids by Lozano et al[8] and have shown emission stability, but a low thrust per emission site (in the order of

Copyright © 2023 by First Author. Posted on line by the EUCASS association with permission.

DOI: 10.13009/EUCASS2023-985

0.1 μN[13]). The solution to this problem is to create an array of emission sites to accommodate for a larger liquid flow rate. The main drawback of externally wetted emitters is the difficulty of flow control, since it is passively controlled through the viscosity of the liquid, μ, and geometric parameters of the emitter, the most important being the surface roughness.[14] These two parameters control the hydraulic impedance, R_H,

$$R_H = \frac{\mu}{2\pi K_{\text{ps}} \sin\theta} \ln\left(\frac{h_c}{R_c}\right) \tag{1}$$

where K_{ps} is the permeability of the surface layer [m^3], θ is the cone semiangle, R_c is the base of emission region and it is typically of the order of $10^{-1} - 10^{-2}$ μm,[15] and h_c the height of the emitter. From this equation, it is clear that for a fixed emitter geometry (K_{ps}, θ, R_c, and h_c), the flow rate is driven by the viscosity of the liquid. If the viscosity decreases, the hydraulic impedance decreases, hence increasing the flow rate, Q.

In electrospray thrusters, controlling the flow rate is essential to achieve pure ionic regime, as the flow rate per emission site needs to be restricted below a critical flow rate for the particles to be extracted without the formation of droplets.[10] This minimum flow rate depends solely on the liquid properties.[16] In addition to restraining the flow rate, the electric field needs to be strong enough for ions to be evaporated. The maximum electric field that can be attained on the surface of the emission site also depends on the liquid properties, with electrical conductivity (K) and surface tension (γ) being the most important parameters. For an externally wetted emitter, the higher K and γ, the higher the electric field that can be attained and the higher the current than can be emitted, facilitating pure ionic regime.[17] On the other hand, a high μ results in higher hydraulic impedance, hence lower flow rate, which enables attainment of pure ionic regime.

As qualitatively described, the properties of the ionic liquid play a significant role in influencing the emission regime and overall performance of an electrospray thruster. Therefore, carefully selecting or designing an ionic liquid propellant is key to obtained the desired performance. The most common and used IL is 1-ethyl-3-methylimidazolium tetrafluoroborate (EMI- BF_4). The first test using EMI-BF_4 in externally wetted emitters was performed by Lozano and Martínez-Sánchez demonstrating pure ionic emission from a tungsten needle.[8] Later, Velásquez-García et al. characterized the current emission from an microfabricated array of needles.[18] There are several reported results on EMI-BF_4 using externally wetted emitters with all of them lying in the pure ionic or near-pure ionic regime.[19,20] Another common liquid in electrospray is 1-ethyl-3-methylimidazolium bis-trifluoromethylsulfonyl-imide (EMI-Im). This liquid has a lower conductivity than EMI-BF_4, but it is much less hygroscopic which improves its use in vacuum.[21] EMI-Im has been extensively tested with capillary emitters showing a great amount of droplets.[22] With externally wetted emitters, Lozano reported pure ionic emission,[23] in contrast to other authors where mixed regime has been observed.[9,24] Another liquid that has been successfully tested with externally wetted emitters is 1-ethyl-3-methylimidazolium dicyanamide (EMI-DCA).[25] EMI-DCA presents a relatively high conductivity and surface tension which should favor a high charge-to-mass emission.

The purpose of this work is to gain understanding of how the properties of the liquid affect the emission characteristics and performance of externally wetted emitters, as well as explore new ionic liquids that could be suitable for electrospray propulsion. In total seven liquids are studied. Three of the seven ILs tested are the widely known throughout the literature and already mentioned EMI-BF_4, EMI-Im and EMI-DCA. The remaining four ILs, to the best of our knowledge, have never been characterized for externally wetted emitters: 1-ethyl-3-methylimadazolium thiocyanate (EMI-SCN),[26] 1-ethyl-3-methylimidazolium triflate (EMI-OTf),[27] 1-ethyl-3-methylimidazolium trifluoromethanesulfonate (EMI-TFA), and 1-ethyl-3-methyl-imidazolium-ethylsulphate (EMI-$EtOSO_3$), of which the last two have not been reported for any emitter topology.

The thruster used throughout this work is an IENAI SPACE prototype (ATHENA).[12] The performance of the thruster will be assessed for different operating voltages at room temperature. A time-of-flight mass spectrometer (ToF) technique, specifically adapted to the characteristics of the thruster, was used to derived the performance. The rest of the article is organized as follows: Sec.2 presents the thruster, the ionic liquids and the experimental set-up, Sec.3 discusses the obtained results and Sec.4 summarizes the conclusions extracted.

2. Experimental methods

2.1 Ionic liquid propellants

A variety of ionic liquids have been selected to characterize their operation, EMI-BF_4, EMI-DCA, EMI-Im, EMI-SCN, EMI-OTf, EMI-TFA, EMI-$EtOSO_3$. They were purchased from IoLiTec with a purity of 99%. The data from liquids like EMI-BF_4 or EMI-Im that have been previously characterized serves as benchmark for testing the rest of the propellants. Table 1 shows the physical properties of the ILs. Among the different ILs studied we find two highly

DOI: 10.13009/EUCASS2023-985

conductive hypergolic liquids (EMI-DCA and EMI-SCN), a low conductivity but high viscosity liquid (EMI-$EtOSO_3$) and four with moderate conductivity (EMI-BF_4, EMI-Im, EMI-OTf and EMI-TFA). The selection of these liquids was to have the same cation (EMI^+), but different anion, with a wide range of different properties to extract as many conclusions as possible from the performance of the liquids.

IL	Anion mass [Da]	γ [mN/m]	K [S/m]	μ [mP s]	ρ [g/cm^3]
EMI-BF_4	87	52	1.4	44	1.29
EMI-Im	282	36	0.9	34	1.52
EMI-DCA	66	61	2.8	15	1.10
EMI-SCN	58	49	1.8	28	1.12
EMI-OTf	150	40	0.9	40	1.39
EMI-TFA	114	-	1.0	29	1.31
EMI-$EtOSO_3$	127	47	0.4	98	1.24

Table 1: Properties of the ionic liquids at room temperature (25 °C).[28–33] Molecular mass of EMI^+ is 112 Da.

2.2 Thruster description

The electrosprays thruster comprises a silicon-based extractor grid and an externally wetted emitter array, both of which are micro-fabricated. The emitter array incorporates 101 micro cones with nano-texturization to facilitate wettability towards the tip and regulates the hydraulic impedance. An schematic of a four emission site emitter with corresponding extractor holes is shown in Figure 1. In addition, the emitter includes multiple feeding holes that allow the ionic liquid to flow passively from the reservoir positioned beneath the emitter to the emission sites. To ensure an uninterrupted liquid connection between the emitter and reservoir, a porous textile material is inserted. The reservoir itself is constructed using 3D printing technology, employing a porous aluminum piece. An schematic of the thruster assembly before testing is shown in Figure.

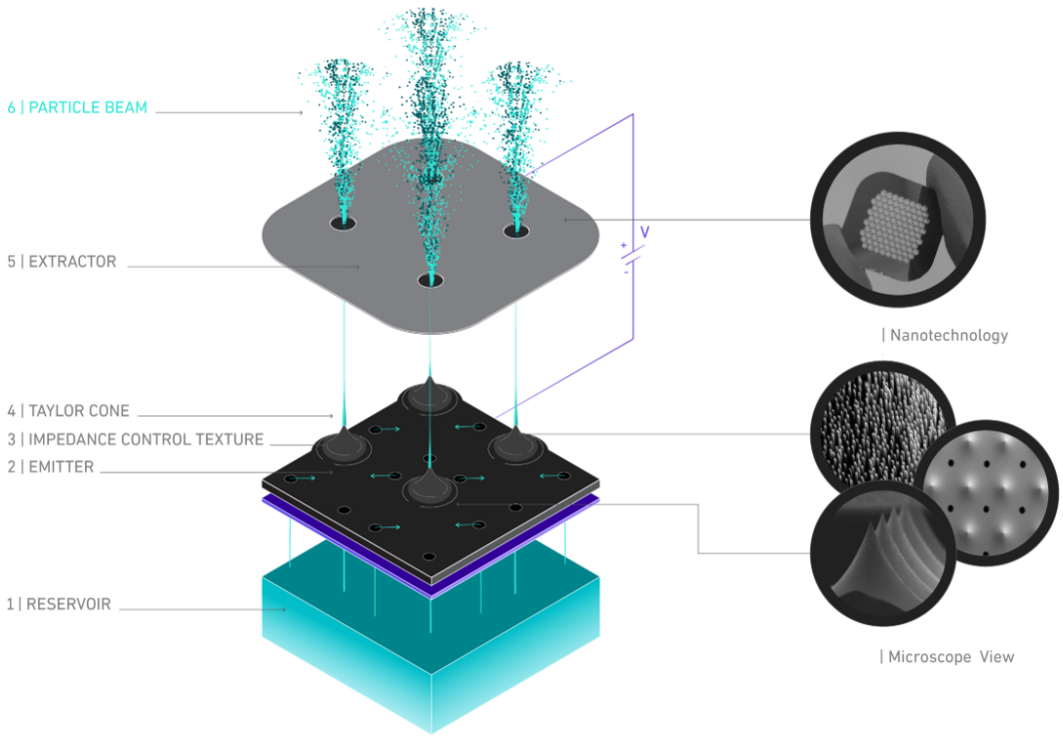

Figure 1: Schematic of thruster assembly.

DOI: 10.13009/EUCASS2023-985

For every propellant a different emitter was used to avoid cross-contamination. Also, all the thrusters used for this test correspond to the same fabrication wafer to reduce repeatability errors. Each emitter has been characterized using a scanning electron microscope to ensure that all the parameters of the emitter lie within the acceptable tolerances. Since each emitter contains 101 emission sites, random mechanical errors in individual tips can be neglected. Moreover, a different reservoir was used for every liquid to avoid contamination. All the reservoirs were filled with the same amount of propellant, 45 μL. To minimize the uncertainty arising from various thrusters, the experimental operations were carried out utilizing an identical procedure for thruster assembly and propellant handling.

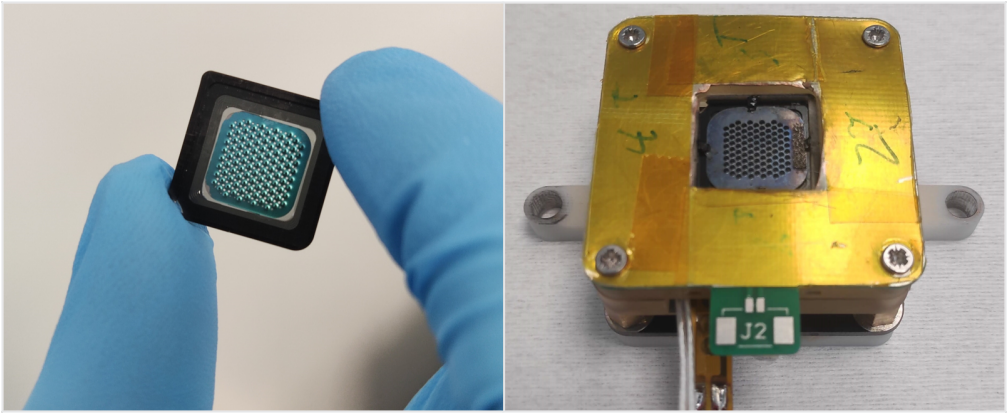

Figure 2: Microfabricated emitter and complete assembly before testing.

2.3 Vacuum facility and diagnostics

The vacuum facility comprises a cube with 290 mm sides, featuring an extension tube that is 775 mm long and has an inner diameter of 97 mm, see Figure 3. Positioned along the central axis of one face of the cube, this setup is equipped with an Edwards 85 L/s turbo-molecular pump to maintain a chamber pressure below 10^{-5} mbar. Refer to Figure 4 for a schematic representation of the experimental arrangement.

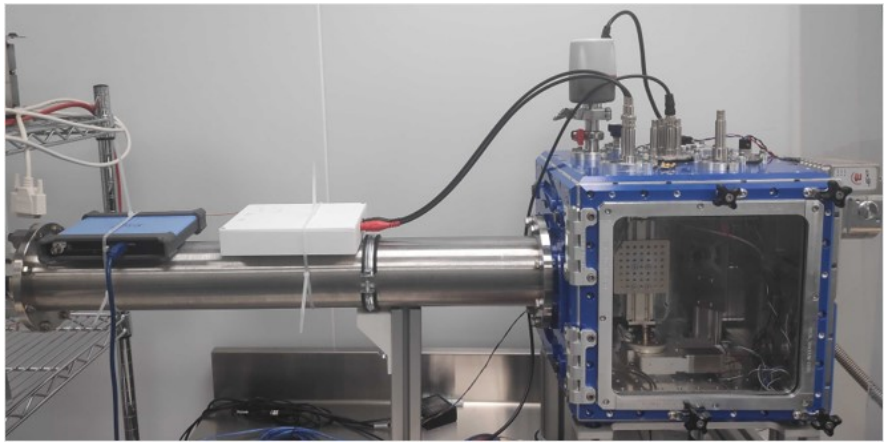

Figure 3: Vacuum chamber with extension tube for TOF measurements.

2.3.1 Time-of-Flight Mass Spectrometry

ToF mass spectrometry plays a vital role in characterizing the composition of the thruster ion beam. It serves as a valuable diagnostic tool in electrospray propulsion, facilitating the identification of different emitted particles and their contributions to the total emitted current. Additionally, it enables the determination of the average specific charge (q/m) and provides an indirect estimation of thrust and specific impulse.

The analysis in ToF mass spectrometers involves measuring a time wave of the charged particle beam current, which is modulated by an electrostatic gate. As the ions traverse a specific flight region denoted as L_{ToF}, their time of flight is measured. The time taken by each particle n can be expressed as:

DOI: 10.13009/EUCASS2023-985

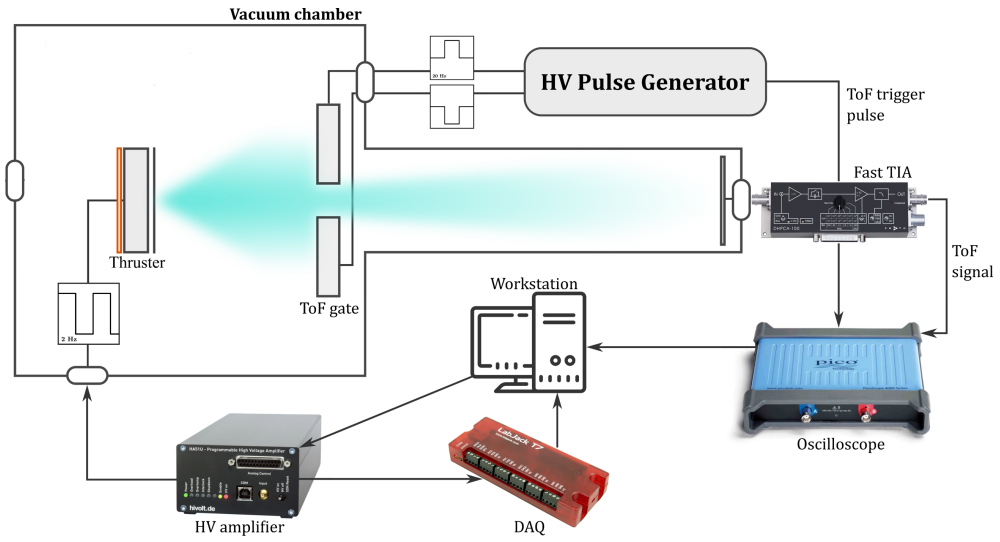

Figure 4: Vacuum system setup schematic.

$$t_n = \frac{L_{\mathrm{ToF}}}{v_n} = \frac{L_{\mathrm{ToF}}}{\sqrt{2(q/m)_n V_a}} \tag{2}$$

where V_a represents the applied voltage. This study utilizes a ToF mass spectrometer similar to other setups described in the literature.[23] It comprises a deflection gate controlled by a high-voltage pulse generator and a collector plate positioned at the end of the flight region. The collected current is then measured using a high-speed trans-impedance amplifier (TIA). Moreover, a secondary electron repeller (SER) is incorporated in front of the collector. Refer to Figure 5 for a schematic representation of the ToF setup.

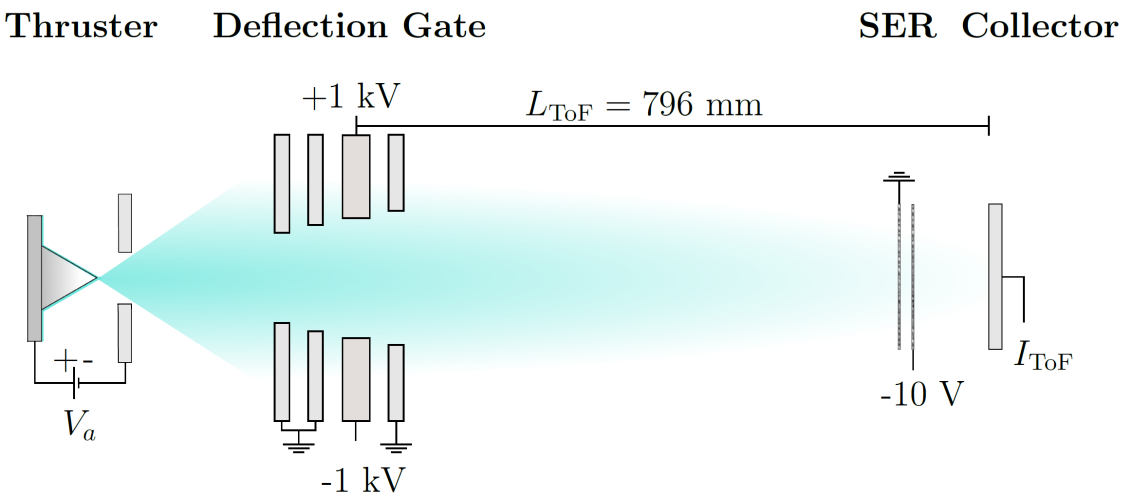

Figure 5: Schematic representation of the electrostatic gate setup in time-of-flight (ToF) mass spectrometry.

The ToF gate functions as an electrostatic shutter and is located near the thruster exit plane. When the electrostatic gate (ESG) is polarized, it deflects all particles upstream, enabling the collection of only downstream particles. Due to variations in specific charges, particles with different velocities reach the collector at distinct times, with those possessing higher velocities arriving first. Figure 6 shows an ideal curve that is arbitrary composed of 40% monomers, 40% dimers, 10% trimers and 10% droplets. The different oligomers correspond to the solvated ions and have fixed q/m, while the droplets are a distribution.

The deflection gate operates by applying an electric field perpendicular to the particle beam, which is generated by two biased plates. With a collection angle of 3.2°, a detector diameter of 90 mm, and a flight length of 796 mm, particles with deflection angles exceeding the collection angle are prevented from reaching the collector, effectively

DOI: 10.13009/EUCASS2023-985

"closing" the gate.

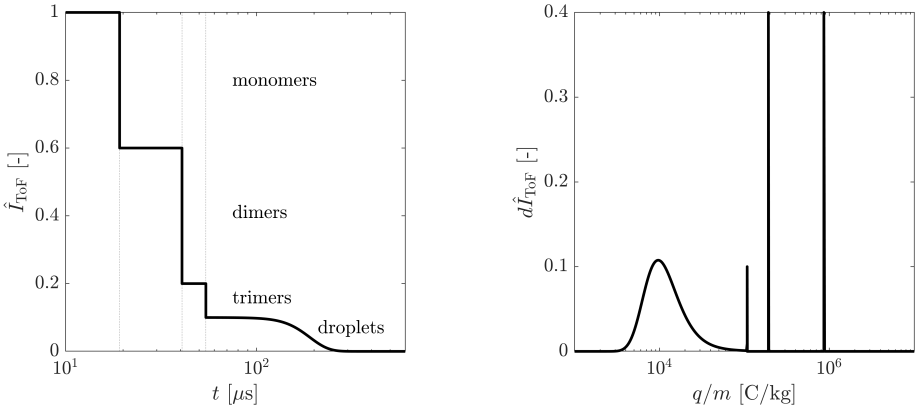

(a) (b)

Figure 6: a) Theoretical ToF timewave for a monoenergetic 1000 V EMI-Im ion beam operating in mixed regime with composition: 40% monomers, 40 % dimers, 10 % trimers and 10 % droplets with an arbitrary m/q distribution, and b) theoretical derivative of the ToF timewave as a function of the specific mass.

The collector is constructed using a 1 mm thick aluminum disk, which is connected to a single-sided BNC feed-through. Positioned 5 mm upstream from the collector, a secondary electron repeller (SER) is installed, consisting of two meshes with 70% transparency and spaced 5 mm apart. The first mesh is directly grounded to the vacuum chamber using conductive tape, while the second mesh is biased to -10V using an external power supply.

To minimize input capacitance and mitigate current noise, a fast trans-impedance amplifier (TIA) is directly connected to the feed-through. In this study, a DHCPA-100 TIA is employed, featuring variable gain and a high bandwidth. The TIA operates in low-noise mode with a gain of 1 MOhm, resulting in a bandwidth of 1.8 MHz. This corresponds to a minimum rise time of 194 ns.

The high-voltage (HV) pulse generator responsible for driving the electrostatic gate (ESG) is a custom-built device based on a design by Horowitz et al.[34] The circuit incorporates two half bridges that alternate the output between a high-voltage level and ground. It has the capability to bias the gate electrodes to ± 1 kV, resulting in a 2 kV differential voltage, with a rise time of 180 ns.

3. Results

3.1 Thruster operation

For each propellant, the thruster was operated using a HV amplifier according to the following procedure:

1. Increasing square wave for emission characterization. A square signal with semi-period of 1 s that increases ±50 V every period. The applied voltage started at 0 V and was increased until 1600 V was reached giving a total of 33 point to construct the I-V curve.

2. To perform the ToF measurements, the thruster was operated with a square timewave at a fixed voltage. At a given voltage, the magnitudes of the current of the positive and negative emission are different depending on the liquid. To avoid charge accumulation with time, the thruster was driven with a square wave in the positive polarity for a fixed time $t^+ = t_1$ and variable duration $t^- = t_2 - t_1$ in the negative polarity until the time integral of the positive and negative emitted currents matches (i.e. $\int_0^{t_1} I_e^+ dt = \int_{t_2}^{t_1} I_e^- dt$). Voltage polarity was changed at a rate of 1 Hz to avoid electrochemical reactions,[35] so that $t^+ = 1$ s and $t^- = t^+ \left(I_e^+ / I_n^-\right)$.

An schematic of the increasing square and the ToF operation square wave used is shown in 7. The time t_2, is updated in real time during each cycle to fulfill the relation. For each propellant, ToF measurements were taken at seven different voltages, from 1000 V to 1600 V in steps of 100 V. The operation temperature was 25 °C during all the tests.

DOI: 10.13009/EUCASS2023-985

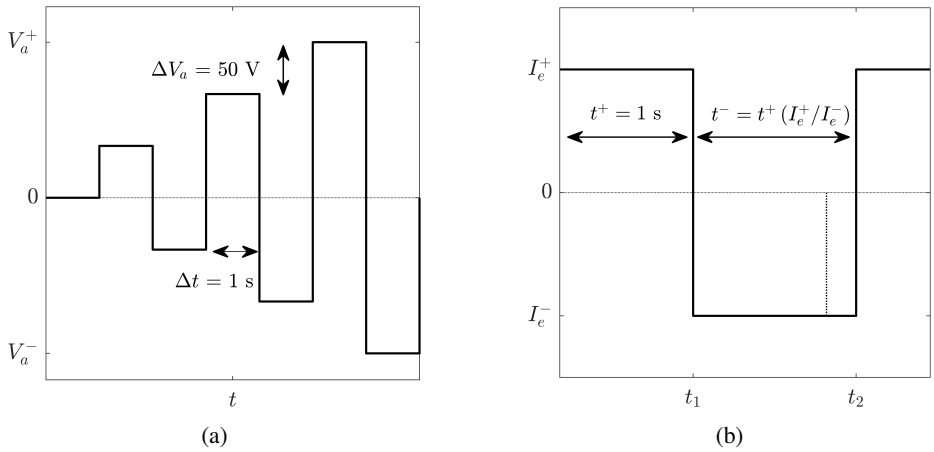

Figure 7: a) Increasing square used to characterize the I-V curve, and b) Current compensation methodology to avoid electrochemical reactions during operation. Positive polarity has a fixed time. Negative polarity has variable time depending on current emission levels.

3.2 Emission characterization

Using the signal from procedure 1, each propellant was tested to extract the I-V curve. Figure 8 shows the emitted currents for each of the ILs at different voltages. Since the cation is the same for all them, for simplicity the legend will only indicate the anion name. It is inferred that the highest the conductivity the higher the emitted current will be, as it was expected. EMI-DCA with $K = 2.8$ S/m shows the highest emitted currents with an average of 490 μA at 1600 V, while the lowest emitted current corresponds to the liquid with the lowest conductivity, EMI-$EtOSO_3$ with $K = 0.4$ S/m, with an average of 61 μA at 1600V. As the conductivity increases in the ionic liquids, the emitted current is increased, as observed by Figure 9.

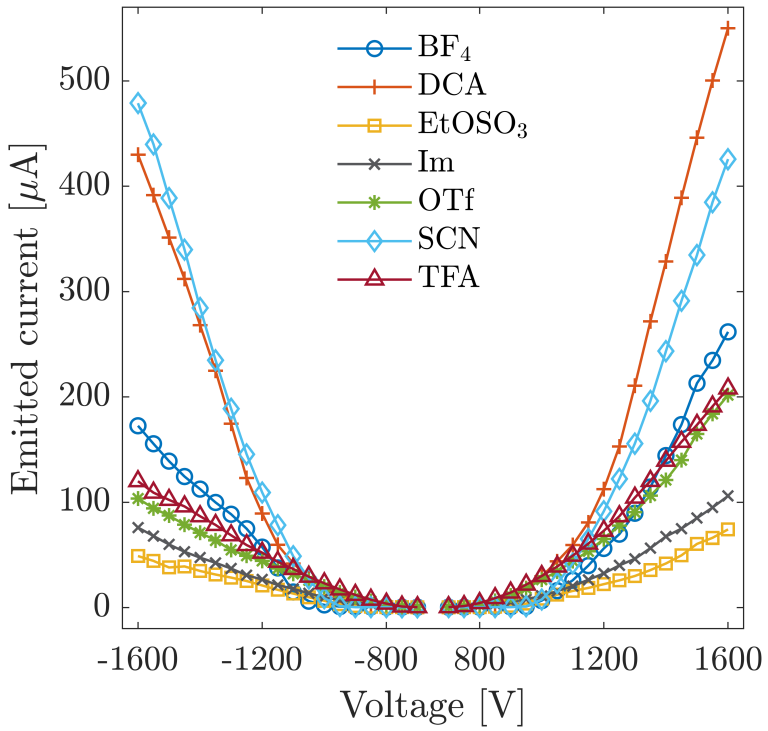

Figure 8: Emitted currents for positive and negative polarities for all the ionic liquids tested.

DOI: 10.13009/EUCASS2023-985

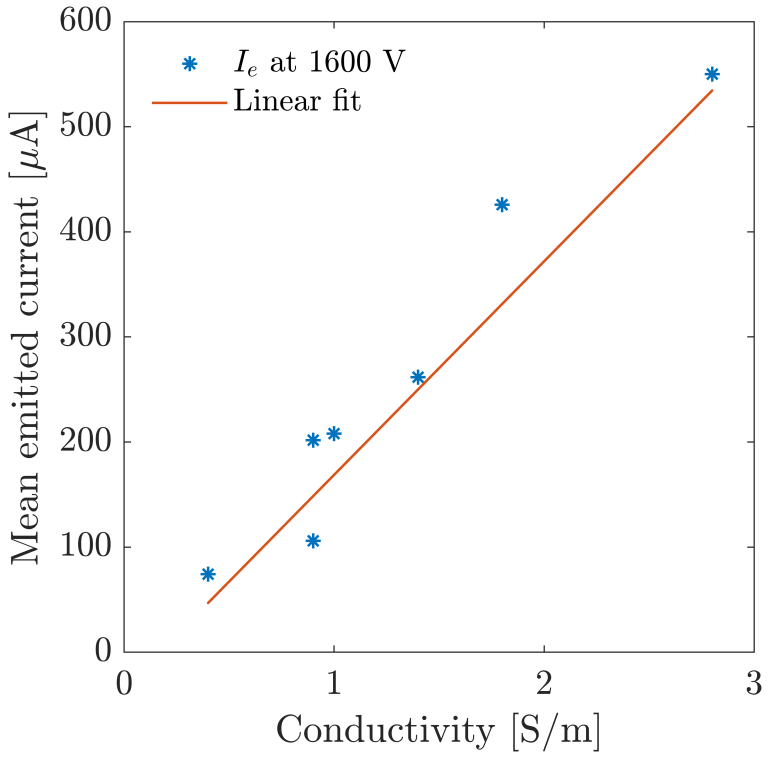

Figure 9: Linear fit of mean emitted current at 1600 V vs conductivity of the ionic liquids.

3.3 Time-of-flight spectra

Throughout the Time-of-Flight (ToF) measurements, the thruster was operated using the square waveform as described in procedure 2 of Section 3.1. The flight times obtained during the measurements are converted into ion masses using Equation 2, assuming that all particles possess a charge of e. This conversion is performed for the sake of convenience in the plots, as the ion masses are known. However, it should be noted that this assumption is technically not applicable to the droplets, whose m/q distribution comprises droplets of varying masses and charges. Each trace presented represents the average of 400 ToF measurements to reduce noise and uncertainty.

ToF measurements are taken from 1000 V to 1600 V in steps of 100 V for positive and negative emission for each liquid, which results in a total of 98 curves. For the sake of simplicity, it will be shown only the ToF spectra at two voltages for positive and negative polarity. To estimate the performance in Section 3.4, all the data points are used. Figure 11 show the ToF curves for the seven liquids and 1000 V and 1600 V, respectively. For each liquid, there are four ToF curves, the top ones show the results during positive emission for both voltages, the the bottom during negative emission.

The two voltages chosen were 1000 V and 1600 V to be able to visually identify differences. Higher voltages enhance ion evaporation which usually results in not only higher emitted currents but a higher fraction of ions respect to droplets. Note the curves at 1000 V are noisier due to the lower collected current at the end of the ToF tube. For all the liquids it can be clearly identify how the fraction of droplets is considerably reduced when increasing the voltage. At 1000 V, all the liquids operate in the mixed regime, with EMI-TFA showing the higher droplet current fraction. At 1600 V, EMI-BF_4, EMI-DCA, and EMI-SCN appear to be in pure ionic regime or close to it. Other liquids like EMI-$EtOSO_3$, EMI-Im, EMI-OTf, and EMI-TFA still lie in the mixed regime at 1600 V, with the negative emission showing slightly higher droplet current fraction than the positive. Another interesting finding is that as the voltage is increased, all the liquids increase the fraction of current associated to monomers opposed to that of dimers and trimers.

An interesting results is that, despite the fact that all liquids share the same cation, EMI^+, not all the liquids show the same amount of this particle in the positive emission ToF curve. It appears that liquids with higher conductivity, such as EMI-DCA or EMI-SCN, are able to extract a higher amount of monomers compared to lower conductivity liquids, with around 80% of DCA^- particles 80% and close to 90% of SCN^- particles.

DOI: 10.13009/EUCASS2023-985

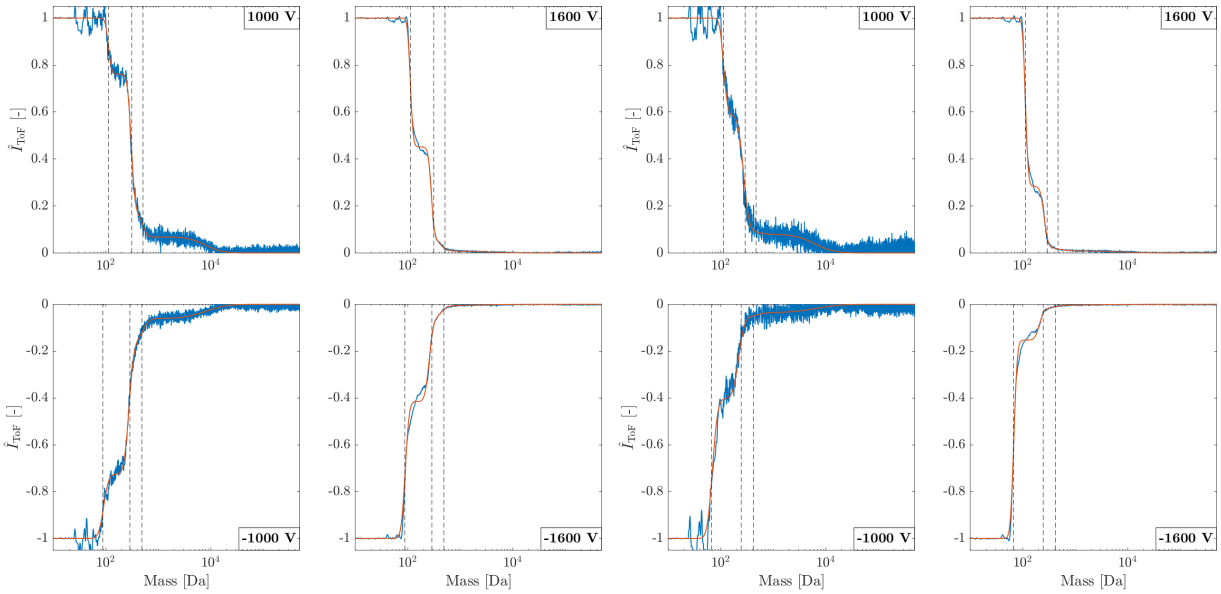

a) EMI-BF_4

b) EMI-DCA

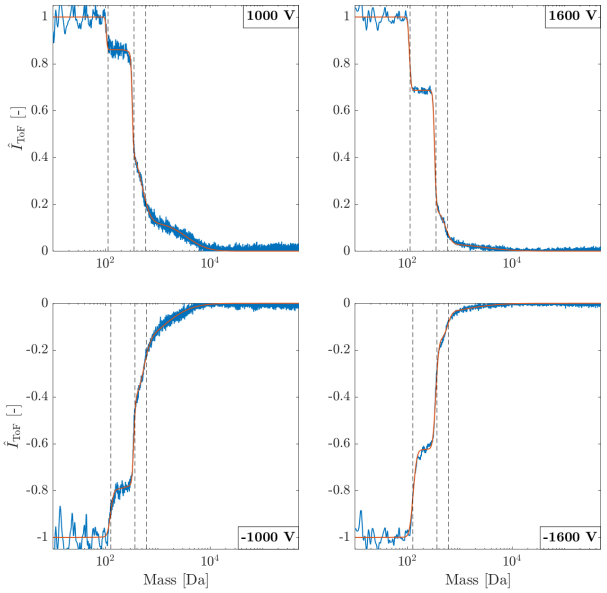

c) EMI-$EtOSO_3$

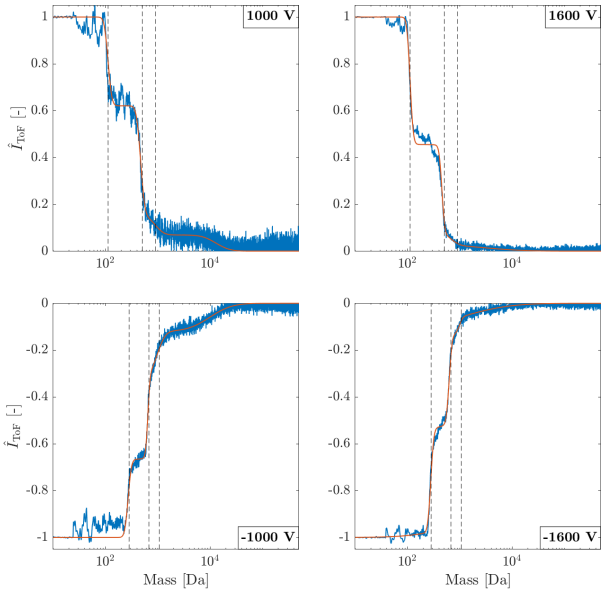

d) EMI-Im

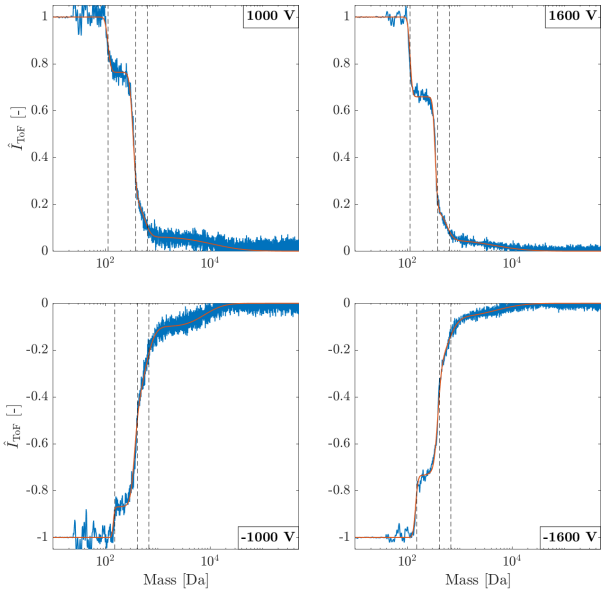

e) EMI-OTf

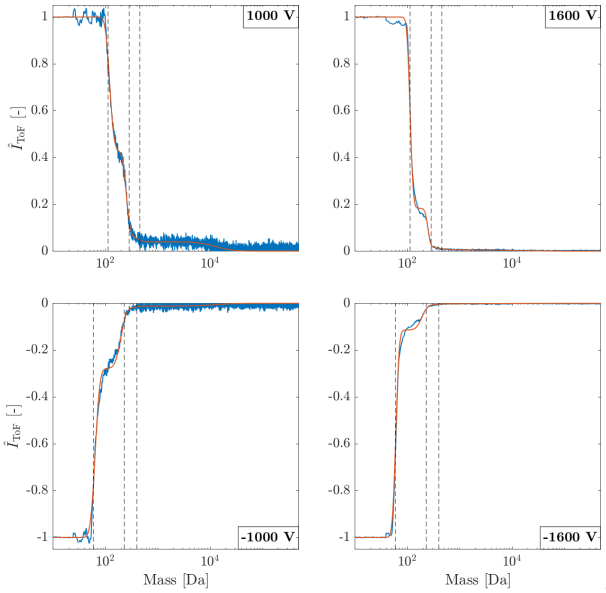

f) EMI-SCN

DOI: 10.13009/EUCASS2023-985

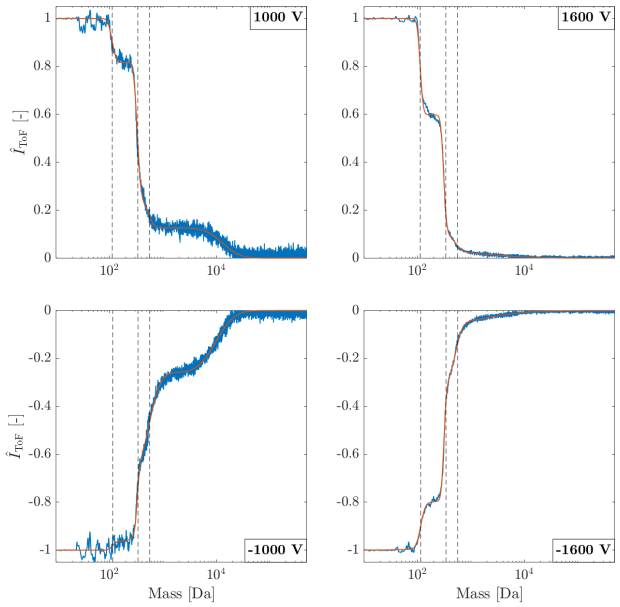

g) EMI-TFA

Figure 11: Experimental time of flight spectra for a) EMI-BF_4, b) EMI-DCA, c) EMI-$EtOSO_3$, d) EMI-Im, e) EMI-OTf, f) EMI-SCN, and g) EMI-TFA for positive and negative emission and two operating voltage 1000 and 1600 V. Dashed lines correspond to the theoretical mass of the oligomers with degree of sovlation $n = 0$ for monomers, $n = 1$ for dimers, and $n = 2$ for trimers. Note that for some of them, trimers are not present at all. Raw data is presented in blue and a fit using log-normal distributions is plotted as the red trace.

3.4 Propulsive performance

By integrating the time of flight curves the thrust and mass flow rate can be obtained. Equation 3 shows the thrust, F_{ToF}, and Equation 4 gives the mass flow,[36]

$$F_{\mathrm{ToF}} = \frac{2V_a I_e}{L_{\mathrm{ToF}}} \int_0^\infty \hat{I}_{\mathrm{ToF}}(t)dt \tag{3}$$

$$\dot{m} = \frac{4V_a I_e}{L_{\mathrm{ToF}}^2} \int_0^\infty t\hat{I}_{\mathrm{ToF}}(t)dt \tag{4}$$

where I_e is the emitted current and $\hat{I}_{\mathrm{ToF}}$ is the normalized ToF curve. Figure 12 shows the performance of the liquid in terms of thrust, specific impulse and thrust efficiency. The thrust efficiency was calculated according to,

$$\eta_T = \eta_\theta \eta_E \eta_p \eta_{tr}^2 \tag{5}$$

where η_θ is the angular efficiency, η_E is the energy efficiency, η_p is the polydispersive efficiency and η_{tr} is the transmission efficiency. All these efficiencies have been characterized for all the liquids and have been taken into account for the thrust efficiency, but are not reported individually. The angular efficiency takes values between 0.8 and 0.9 depending on the liquid and the voltage, energy efficiency remains close to unity ($\sim$ 0.97) and the transmission efficiency was measured >0.99 for all the cases tested. The polydispersive efficiency is calculated according to,

$$\eta_p = \frac{\left(\int_0^\infty \hat{I}_{\mathrm{ToF}}(t)dt\right)^2}{2\int_0^\infty t\hat{I}_{\mathrm{ToF}}(t)dt} = \frac{F_{\mathrm{ToF}}^2}{2\dot{m}I_e V_a} \tag{6}$$

and is a measure of the different species present in the plume and how they are not uniformly accelerated due to the varying q/m. This efficiency is usually the one that penalizes the most the overall thrust efficiency. A plume with only one type of ion particle would have $\eta_p = 1$.

DOI: 10.13009/EUCASS2023-985

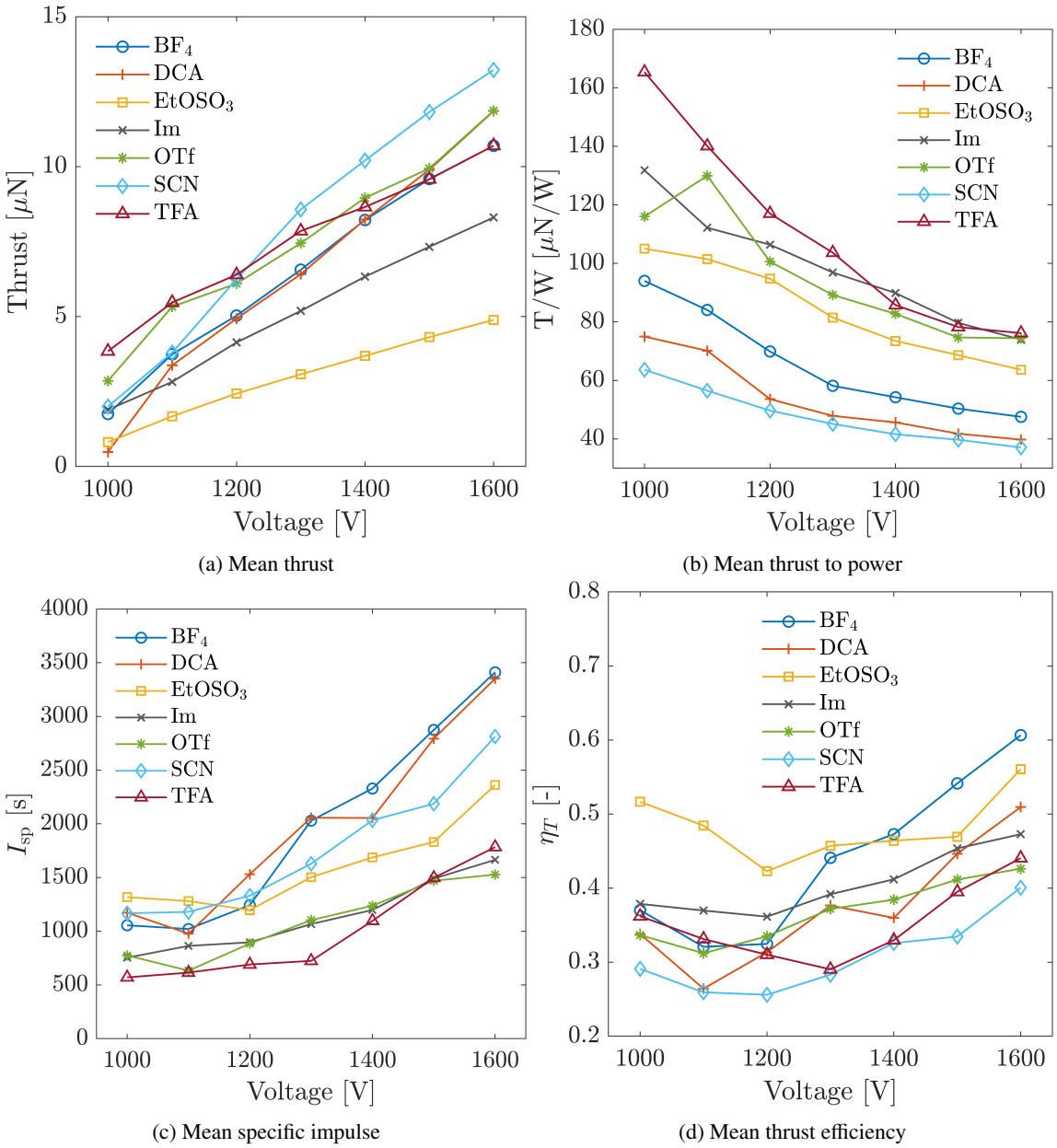

(a) Mean thrust

(b) Mean thrust to power

(c) Mean specific impulse

(d) Mean thrust efficiency

Figure 12: Performance of the seven ionic liquids including a) mean thrust, b) mean thrust to power ratio, c) mean specific impulse, and d) mean thrust efficiency. Note that the mean value is reported as its the weighted averaged between the positive and negative emission.

The thrust increases linearly with voltage. At 1600 V, EMI-SCN shows the highest thrust with 13 μ, while EMI-$EtOSO_3$ the lowest. This is explained by the low emitted current of the latter. Other liquids, like EMI-OTf, even though they do not emit as much as EMI-SCN or EMI-DCA, the presence of droplets (higher mass) in the plume increase the thrust compared to a plume composed of lighter particles.

Since $g_0 I_{sp} = v \propto \sqrt{V_a}$, for a monodisperse specific charge one would expect a square root behavior of I_{sp} as a function of the emitter voltage. However, as was derived of the ToF results, the fraction of droplets and ions varies greatly with voltage and so does the specific mass and polydispersive efficiency resulting in a very different trend. Due to the predominance of droplets at lower voltages (as well as the lower voltage itself) the specific impulse is lower and increases as the voltage increases. From the liquids tested, EMI-BF_4 and EMI-DCA show the highest I_{sp} with values close to 3500 s at 1600V reaffirming that the the liquids are operating in the ionic regime. EMI-SCN shows a slightly lower I_{sp} (2800 s at 1600 V), due to the presence of few droplets with high mass (>10^4 Da). The presence of these droplet could explain also the higher thrust observed. EMI-Im, EMI-TFA and EMI-OTf produce the lowest I_{sp} with values close to 1500 s at 1600 V. These liquids still show droplets at higher voltages, which penalizes significantly the

DOI: 10.13009/EUCASS2023-985

I_{sp}. An interesting case is EMI-$EtOSO_3$ with 2400 s at 1600 V. Despite the fact that the ToF curves still show droplets at higher voltages, the droplets produced are lighter than those of the other liquids (<10^4 Da), generating faster droplets and obtaining a higher specific impulse.

The effect of increasing the voltage and shifting the operating regime from mixed (efficiency penalty) to ionic regime is observed for all liquids, which show the highest values at 1600 V. EMI-BF_4 shows the highest thrust efficiency with 0.6, while EMI-SCN has the lowest efficiency with 0.4 (probably due to the presence of droplets). The faster droplets mentioned for EMI-$EtOSO_3$ are probably the reason why, despite having droplets, the liquid shows a relatively higher efficiency, 0.56, compared to other liquids that also present droplets, 0.47 for EMI-Im and 0.42 for EMI-OTf and EMI-TFA.

4. Conclusions

Seven ionic liquids have been tested and characterized to assess their propulsive performance. The liquids EMI-$BF4_4$, EMI-DCA and EMI-Im serve as benchmark to compare with other research and thruster that have used these liquids. To the best of our knowledge, this is the first report on externally wetted emitters with the liquids EMI-OTf and EMI-SCN. Also, this work characterizes EMI-$EtOSO_3$ and EMI-TFA for the first time for any emitter topology.

The highest emitted current has been observed with liquids with the highest conductivity, EMI-DCA and EMI-SCN. The lowest emitted current was the one of EMI-$EtOSO_3$ as it has the lowest conductivity.

From the ToF data, at lower voltages all the liquids operated in mixed regime. At 1600 V, EMI-BF_4, EMI-DCA and EMI-SCN operate in pure ionic regime, while EMI-Im, EMI-OTf, EMI-$EtOSO_3$, and EMI-TFA still operate in mixed regime.

As for the propulsive performance, the highest thrust was EMI-SCN with 13 μN. EMI-$EtOSO_3$ had the lowest due to the little emitted current. Moreover, those liquids operating in ionic regime present the highest specific impulse with EMI-BF_4 and EMI-DCA yielding the highest with 3450 s. Liquids that operate in mixed regime have a lower value, with EMI-Im, EMI-OTf and EMI-TFA having an specific impulse around 1500 s. EMI-$EtOSO_3$ presents a higher I_{sp} despite operating in mixed regime because the droplets were identified to be lighter. This is speculated that could be because of the higher liquid viscosity. Regarding thrust efficiency, EMI-BF_4 shows the highest with 0.6 at 1600 V, while EMI-SCN has the lowest with 0.4.

Liquids with higher conductivity and surface tension have an advantage in reaching ionic regime at room temperature, as it has been demonstrated with EMI-BF_4, EMI-DCA and EMI-SCN. They are also the only liquids which anion mass is smaller than the cation mass. In fact, the liquids that are reported to operate in the mixed regime, generally show a greater amount of droplets during negative emission, indicating that a high molecular mass could be a reason for droplet formation.

Also, it is of great importance to take into account that these test were conducted at room temperature. In the case of a temperature increase, the viscosity will lower its value, reducing the hydraulic impedance and producing higher flow rates, which will increase the amount of droplets. EMI-$EtOSO_3$ would be a potential candidate to test at higher temperatures. This could solve one of the issues of this liquid which is the low emitted current (due to the low conductivity), while maintaining a viscosity that is high enough to restrain the flow rate. Also, EMI-DCA and EMI-SCN are of great interest since they are hypergolic liquids, so that they could be potentially used in a dual propulsion system (chemical + electrical).

5. Acknowledgments

This work was supported by the "Comunidad de Madrid" under "Ayudas destinadas a la realización de doctorados industriales" program IND2020/TIC-17316.

DOI: 10.13009/EUCASS2023-985

References

[1] Akshay Reddy Tummala and Atri Dutta. An overview of cube-satellite propulsion technologies and trends. *Aerospace*, 4(4):58, 2017.

[2] David Krejci, Marco Gomez Jenkins, and Paulo Lozano. Staging of electric propulsion systems: Enabling an interplanetary cubesat. *Acta Astronautica*, 160:175–182, 2019.

[3] Paulo Lozano and Manuel Martínez-Sánchez. Ionic liquid ion sources: characterization of externally wetted emitters. *Journal of colloid and interface science*, 282(2):415–421, 2005.

[4] J Fernández De La Mora. The effect of charge emission from electrified liquid cones. *Journal of Fluid Mechanics*, 243:561–574, 1992.

[5] Juan Fernández de la Mora, Gary J Van Berkel, Christie G Enke, Richard B Cole, Manuel Martínez-Sánchez, and John B Fenn. Electrochemical processes in electrospray ionization mass spectrometry. *Journal of Mass Spectrometry*, 35(8):939–952, 2000.

[6] Jorge Alejandro Carretero Benignos. *Numerical simulation of a single emitter colloid thruster in pure droplet cone-jet mode*. PhD thesis, Massachusetts Institute of Technology, 2005.

[7] Paulo Lozano and Manuel Martinez-Sanchez. Experimental measurements of colloid thruster plumes in the ion-droplet mixed regime. In *38th AIAA/ASME/SAE/ASEE Joint Propulsion Conference & Exhibit*, page 3814, 2002.

[8] Paulo Lozano and Manuel Martínez-Sánchez. Ionic liquid ion sources: characterization of externally wetted emitters. *Journal of colloid and interface science*, 282(2):415–421, 2005.

[9] Yu-Hui Chiu, Geraldine Gaeta, Thomas Heine, Rainer Dressler, and Dale Levandier. Analysis of the electrospray plume from the emi-im propellant externally wetted on a tungsten needle. In *42nd AIAA/ASME/SAE/ASEE Joint Propulsion Conference & Exhibit*, page 5010, 2006.

[10] Ignacio Romero-Sanz, Rodrigo Bocanegra, J Fernandez De La Mora, and M Gamero-Castano. Source of heavy molecular ions based on taylor cones of ionic liquids operating in the pure ion evaporation regime. *Journal of Applied Physics*, 94(5):3599–3605, 2003.

[11] David Krejci, Fernando Mier-Hicks, Robert Thomas, Thomas Haag, and Paulo Lozano. Emission characteristics of passively fed electrospray microthrusters with propellant reservoirs. *Journal of Spacecraft and Rockets*, 54(2):447–458, 2017.

[12] David Villegas-Prados. Impact of the propellant temperature on the performance of externally wetted electrospray thrusters. In *International Electric Propulsion Conference Boston*, 2022.

[13] Robert S Legge Jr. *Fabrication and characterization of porous metal emitters for electrospray applications*. PhD thesis, Massachusetts Institute of Technology, 2008.

[14] Blaise Gassend, Luis Fernando Velasquez-Garcia, Akintunde Ibitayo Akinwande, and Manuel Martínez-Sánchez. A microfabricated planar electrospray array ionic liquid ion source with integrated extractor. *Journal of Microelectromechanical Systems*, 18(3):679–694, 2009.

[15] Chase Coffman, Manuel Martínez-Sánchez, FJ Higuera, and Paulo Lozano. Structure of the menisci of leaky dielectric liquids during electrically-assisted evaporation of ions. *Applied Physics Letters*, 109(23):231602, 2016.

[16] Alfonso M Gañán-Calvo, N Rebollo-Muñoz, and JM Montanero. The minimum or natural rate of flow and droplet size ejected by taylor cone–jets: physical symmetries and scaling laws. *New Journal of Physics*, 15(3):033035, 2013.

[17] C Larriba, D Garoz, C Bueno, I Romero-Sanz, S Castro, Juan Fernández de la Mora, Y Yoshida, G Saito, R Hagiwara, K Matsumoto, et al. Taylor cones of ionic liquids as ion sources: The role of electrical conductivity and surface tension. *ChemInform*, 39(42):no–no, 2008.

[18] Luis Fernando Velásquez-García, Akintunde Ibitayo Akinwande, and Manuel Martinez-Sanchez. A planar array of micro-fabricated electrospray emitters for thruster applications. *Journal of Microelectromechanical Systems*, 15(5):1272–1280, 2006.

DOI: 10.13009/EUCASS2023-985

[19] Chengjin HUANG, LI Jianling, and LI Mu. Performance measurement and evaluation of an ionic liquid electrospray thruster. *Chinese Journal of Aeronautics*, 2021.

[20] Michael R Natisin and Henry L Zamora. Performance of a fully conventionally machined liquid-ion electrospray thruster operated in pir. In *Proceedings of the 36th International Electric Propulsion Conference, Vienna, Austria*, pages 9–12, 2019.

[21] David Conroy and John Ziemer. Water contaminant mitigation in ionic liquid propellant. 2009.

[22] Manuel Gamero-Castaño. Characterization of the electrosprays of 1-ethyl-3-methylimidazolium bis (trifluoromethylsulfonyl) imide in vacuum. *Physics of Fluids*, 20(3):032103, 2008.

[23] Paulo C Lozano. Energy properties of an emi-im ionic liquid ion source. *Journal of Physics D: Applied Physics*, 39(1):126, 2005.

[24] Brian Ticknor, Shawn Miller, and Yu-Hui Chiu. Mass spectrometric analysis of the electrospray plume from an externally wetted tungsten ribbon emitter. In *45th AIAA/ASME/SAE/ASEE Joint Propulsion Conference & Exhibit*, page 5088, 2009.

[25] Chengjin Huang, Jianling Li, and Mu Li. Experimental characterization of the electrospray propulsive performance for ionic liquid propellants [emim][dca] and [bmim][dca]. *Fuel*, 336:126822, 2023.

[26] Charles Ryan, A Daykin-Iliopoulos, John Stark, Anna Salaverri, Ernesto Vargas, Pelle Rangsten, Simon Dandavino, Caglar Ataman, Subha Chakraborty, Daniel Courtney, et al. Experimental progress towards the microthrust mems electrospray electric propulsion system. In *33rd International Electric Propulstion Conference*, number CONF, 2013.

[27] Navin Timilsina. *Electrospray Thrusters for Attitude Control of a 1-U CubeSat*. University of California, Irvine, 2014.

[28] Suojiang Zhang, Xingmei Lu, Qing Zhou, Xiaohua Li, Xiangping Zhang, and Shucai Li. *Ionic liquids: physicochemical properties*. Elsevier, 2009.

[29] W Martino, J Fernandez De La Mora, Y Yoshida, G Saito, and J Wilkes. Surface tension measurements of highly conducting ionic liquids. *Green Chemistry*, 8(4):390–397, 2006.

[30] Ya-Hung Yu, Allan N Soriano, and Meng-Hui Li. Heat capacities and electrical conductivities of 1-ethyl-3-methylimidazolium-based ionic liquids. *The Journal of Chemical Thermodynamics*, 41(1):103–108, 2009.

[31] José S Torrecilla, Tatiana Rafione, Julián García, and Francisco Rodríguez. Effect of relative humidity of air on density, apparent molar volume, viscosity, surface tension, and water content of 1-ethyl-3-methylimidazolium ethylsulfate ionic liquid. *Journal of Chemical & Engineering Data*, 53(4):923–928, 2008.

[32] Oscar Nordness, Luke D Simoni, Mark A Stadtherr, and Joan F Brennecke. Characterization of aqueous 1-ethyl-3-methylimidazolium ionic liquids for calculation of ion dissociation. *The Journal of Physical Chemistry B*, 123(6):1348–1358, 2019.

[33] Hector Rodriguez and Joan F Brennecke. Temperature and composition dependence of the density and viscosity of binary mixtures of water+ ionic liquid. *Journal of Chemical & Engineering Data*, 51(6):2145–2155, 2006.

[34] Paul Horowitz, Winfield Hill, and Ian Robinson. *The art of electronics*, volume 2. Cambridge university press Cambridge, 1989.

[35] Paulo Lozano and Manuel Martínez-Sánchez. Ionic liquid ion sources: suppression of electrochemical reactions using voltage alternation. *Journal of colloid and interface science*, 280(1):149–154, 2004.

[36] Elaine Petro, Amelia Bruno, Paulo Lozano, Louis E Perna, and Dakota Freeman. Characterization of the tile electrospray emitters. In *Aiaa propulsion and energy 2020 forum*, page 3612, 2020.